MIT Libraries | DSpace@MIT

MIT Open Access Articles

# *Ultra-low-power electronics for non-invasive medical monitoring*

The MIT Faculty has made this article openly available. ***Please share*** how this access benefits you. Your story matters.

**Citation:** Turicchia, L. et al. "Ultra-low-power Electronics for Non-invasive Medical Monitoring." IEEE, 2009. 85–92. © Copyright 2012 IEEE

**As Published:** http://dx.doi.org/10.1109/CICC.2009.5280892

**Publisher:** Institute of Electrical and Electronics Engineers (IEEE)

**Persistent URL:** http://hdl.handle.net/1721.1/71794

**Version:** Final published version: final published article, as it appeared in a journal, conference proceedings, or other formally published context

**Terms of Use:** Article is made available in accordance with the publisher's policy and may be subject to US copyright law. Please refer to the publisher's site for terms of use.

Massachusetts Institute of Technology

*Invited Paper*

# Ultra-low-power Electronics for Non-invasive Medical Monitoring

L. Turicchia[1], S. Mandal[1], M. Tavakoli[2], L. Fay[3], V. Misra[4], J. Bohorquez[1], W. Sanchez[1], and R. Sarpeshkar[1]
(1) Department of Electrical Engineering and Computer Science, Massachusetts Institute of Technology, Cambridge, MA 02139.
(2) Linear Technology Corporation, North Chelmsford, MA 01863
(3) SRI International, Menlo Park, CA 94025.
(4) Department of Electrical Engineering, Stanford University, Stanford, CA 94305.

***Abstract*-New electronics for non-invasive medical monitoring promise low-cost, maintenance-free, and lightweight devices. These devices are critical in long-term medical measurements and in home-based tele-monitoring services, which are extremely important for the reduction of health care costs. Here, we present several methods for reducing power consumption while retaining precision. In particular, we focus on the monitoring of the heart—because of its importance—and we describe a micropower electrocardiograph, an ultra-low-power pulse oximeter, an ultra-low-power phonocardiograph, an integrated-circuit switched-capacitor model of the heart, and a low-power RF-antenna-powered CMOS rectifier for energy harvesting. We also introduce an ultra-low-power platform for medical monitoring that enables the integration of monitoring circuitry in a wireless, low-cost, and battery-free device, and describe a method for audio localization of the device in case of a medical alarm.**

## I. Introduction

Heart disease is the most common disease in developed countries. According to the National Center for Health Statistics, 29% of adult Americans have hypertension and an additional 28% have prehypertension [1]. Consequentially, monitoring the cardiovascular system of almost every person in the United States has become important. In addition, heart-disease management plays a major role among health-care policies due to the high cost of treating this disease. According to the American Heart Association, heart-failure patient care cost $24 billion in the United States in 2003, with hospitalization accounting for 70% of this expense [2]. As pointed out by the Home-Care Management Systems study (TEN-HMS) cost reduction can be achieved using home-based telemonitoring services for heart-failure patients [2]. This cost saving is primarily due to the fact that home telemonitoring patients spend fewer days in the hospital than normal patients. In addition, home telemonitoring has also led to very high patient satisfaction [2]. Therefore, there is a considerable interest in finding wearable monitoring devices that can be comfortably used by patients at home. This interest provides new motivation for the development of low-power non-invasive medical-monitoring devices, which in the past were only used for measurements not achievable in a hospital (e.g., long term monitoring of the heart). Nowadays, these devices are seen as one of the best technologies for reducing skyrocketing health care costs.

Research on electronics for non-invasive medical monitoring has been focused on reducing the overall power consumption of such devices. In fact, power consumption is the most critical limitation of previous realizations, which have batteries that are too heavy to be wearable and/or that needed to be constantly recharged. The cost of the battery is also a key limiting factor for the widespread adoption of this technology. In this article, we summarize some innovations carried out by our group toward non-invasive medical monitoring devices that are free from the weight, cost, and recharging needs of batteries. To achieve this goal, we developed four kinds of components: (1) ultra-low-power sensor circuits able to transduce and amplify the medical signal of interest, (2) a circuit model of the medical system from which we want to infer relevant properties, (3) a low-power CMOS rectifier able to convert ambient radio frequency power to energy utilizable by our device, and (4) an ultra-low-power platform—comprising an antenna and logic circuitry—that allows event processing, energy harvesting, and communication with other devices.

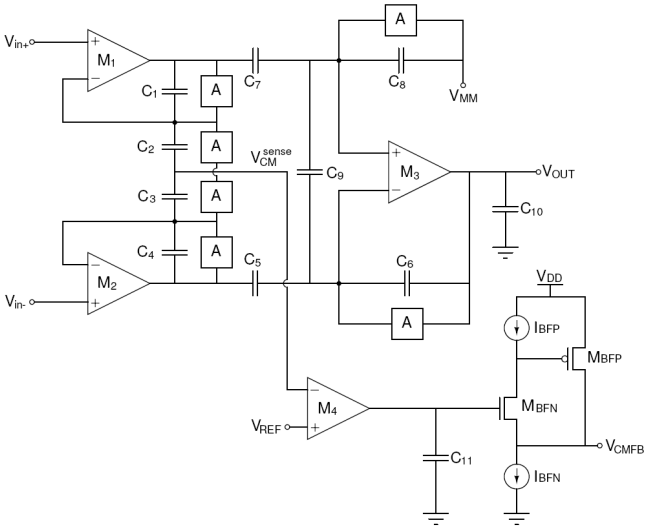


Fig. 1. Electrocardiogram amplifier schematic.

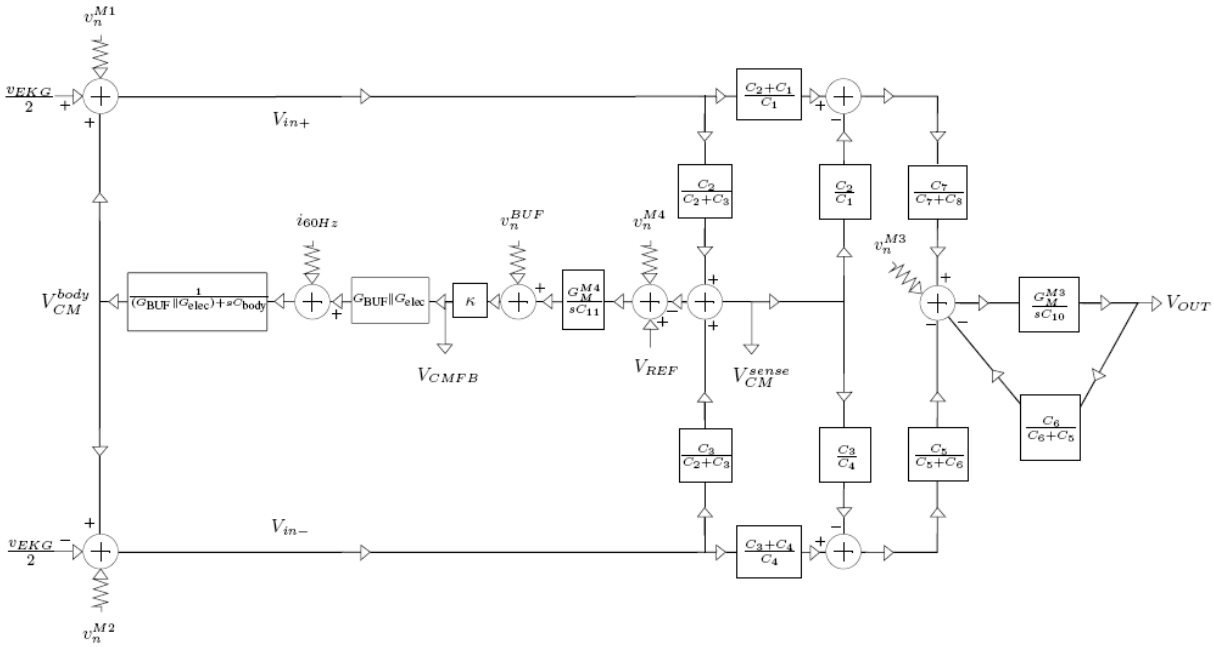


Fig. 2. Block diagram of the EKG amplifier. Jagged arrows denote noise sources.

This paper is organized as follows: In Section II, III, and IV, we describe the design of a micropower electrocardiograph, an ultra-low-power pulse oximeter, and an ultra-low-power phonocardiograph, respectively. In Section V, we present an integrated-circuit switched-capacitor model and implementation of the heart. In Section VI we describe the design of a low-power RF-antenna-powered CMOS rectifier. In Section VII, we present an ultra-low-power battery-free platform for wireless medical monitoring. In Section VIII, we conclude by summarizing our contributions.

## II. A Micropower Electrocardiograph

The electrocardiogram (EKG or ECG)—the recording of the electrical activity of the heart over time—is one of the fundamental components in a medical-monitoring setup because it allows important diagnostic analysis of the heart's functionality. In its simplest circuit implementation, the EKG is a high-input-impedance differential amplifier with high Common-Mode Rejection Ratio (CMRR) and ~μV input-referred noise—needed because the high-impedance input nodes pick up a great amount of interfering common-mode 60Hz signal and P-waves in EKG signals are faint. The design of such amplifiers with a micropower budget and without stringent matching requirements is hard.

Fig. 1 shows our micropower EKG amplifier schematic. It is based on a standard two-gain-stage instrumentation-amplifier topology. The topology has common-mode feedback to create an 'active ground' that is effective in suppressing 60Hz noise [12] and obviates the need for extremely stringent matching needed in purely feedforward designs. In this scheme, $V_{in+}$ and $V_{in-}$ are connected to the input electrodes, $V_{CMFB}$ corresponds to the ground electrode, and $V_{OUT}$ is the amplifier output. In the final implementation, the amplifiers $M_1$, $M_2$, $M_3$, and $M_4$ are 5-transistor pFET-differential-pair operational transconductance amplifiers (OTAs). The first-stage amplifier ($M_1$, $M_2$) uses a 1.5V supply while $M_3$ and $M_4$ operate at 3V. The dual supply is implemented via outputs from different stages of a charge pump in an energy-harvesting antenna design [11] or by simple series stacking of 1.5V cells in battery-based designs.

This amplifier was fabricated in an AMI 0.5μm process and has a total power consumption of 2.76μW, 8.1μVrms input-referred noise, 45.3dB gain, 290Hz bandwidth, 41.8 dB dynamic range, and CMRR (at 60Hz) of 90dB. This amplifier is, to our knowledge, the lowest power EKG amplifier built so far. In fact, current active-grounding EKG amplifier designs consume 20μW or more [3]. Purely feed-forward strategies require high differential matching and are relatively costly.

The power reduction is due to eight design choices: (1) the usage of subthreshold transistor operation to improve noise efficiency; (2) the usage of active grounding with common-mode feedback (CMFB) [12]; (3) the usage of gain-setting capacitors in parallel with 'adaptive elements' (shown as the 'A' blocks in Fig. 1 and functioning as back-to-back diodes) instead of resistors [4]; (4) the usage of half-rail supply operation wherever possible (the half-rail supply saves power when extra headroom is unnecessary while full-rail supply increases dynamic range at the output and helps accommodate the input common-mode operating range); (5) optimization of the power allocations amongst amplifier blocks; (6) optimization of the sizing of devices to improve matching and reduce noise; (7) the usage of pFET input devices for all amplifiers to minimize 1/f noise; and (8) the usage of a super source-follower (SSF) [5] as revealed by the transistor-and-current-source circuit of Fig. 1 for obtaining low output impedance, useful in quenching 60 Hz interference signals.

A feedback block diagram that represents all sources of signal and noise of our EKG amplifier is shown in Fig. 2. All the theoretical properties of the amplifier can be derived by analyzing this block diagram. Notice that the $\kappa$ parameter corresponds to the subthreshold exponential constant of transistor $M_{BFN}$, $G_{elec}$ is the electrode admittance (supposed conductive for simplicity), and $G_{BUF}$ is the output conductive of the CMFB buffer.

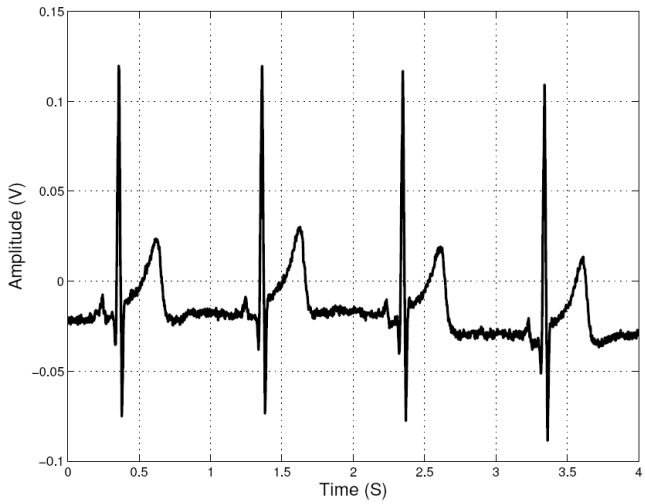


Fig. 3. An example EKG signal captured with the amplifier from a subject with a healthy heart.

The major power reduction achieved by our design does not compromise the quality of the measurements. Fig. 3 shows EKG measurements obtained from a healthy subject using FS-TB1 hydrogel electrodes from Skintact attached to a leg and both arms, and connected to the corresponding terminals of the EKG amplifier. The captured EKG waveform has good SNR and the 'P' waves are clear.

## III. An Ultra-Low-Power Pulse Oximeter

Pulse oximetry is a method for monitoring the oxygen saturation ($S_pO_2$) of a patient's hemoglobin molecules. Oxygen saturation provides a comprehensive measurement of the patient's cardio-respiratory health status. Pulse oximeters measure variations in the optical density of transmission in the arteries due to their contraction and relaxation as a function of time. A pulse-oximeter output waveform is known as a photo-plethysmogram, or PPG. Pulse-oximeter measurements involve the creation of intense flashes of light that make PPG recording very expensive in term of power consumption and consequently impractical for wearable patient monitoring.

We addressed this expensive power budget by developing an ultra-low-power pulse oximeter that achieves more than an order-of-magnitude reduction in power consumption over the best commercial pulse oximeters. This power reduction is due to the creation of a novel logarithmic transimpedance amplifier that eliminates the need for bright LED light. Our design is based on the standard logarithmic transimpedance photoreceptor [4] with the addition of three major improvements: (1) the gain of the amplifier in the photoreceptor is distributed over many stages to increase its gain-bandwidth product for a given power consumption; (2) the addition of an adaptive—loop-gain mechanism to automatically adjust loop gain based on the light intensity, obtaining less speedup for high light levels (to prevent potential instability) and more speedup for low light levels (to achieve larger bandwidth); (3) the usage of a common-gate stage for sensing the input photocurrent and converting it to a logarithm, exploiting the method of unilateralization for speeding up feedback-amplifier response. Details on a preliminary version of the oximeter are described in a thesis [6].

Fig. 4 shows a block diagram of our pulse oximeter system. The input to the chip is a photocurrent coming from a probe connected to the patient and the output of the chip is a current directly proportional to measured oxygen saturation of the patient's hemoglobin molecules. The light needed in the pulse oximeter is provided by two LEDs with red and infrared light. The LEDs are drived by a square wave with a small duty cycle. Both LEDs are alternatively illuminated and the photocurrent generated by a single photodiode is split, switched, and steered into two different paths, one channel sensitive to the red light and the other to IR light. The signals are then amplified by our novel transimpedance amplifiers, low-pass filtered, and divided. Details on the signal processing needed to obtain oxygen saturation from the measured photodiode current can be found in [6].

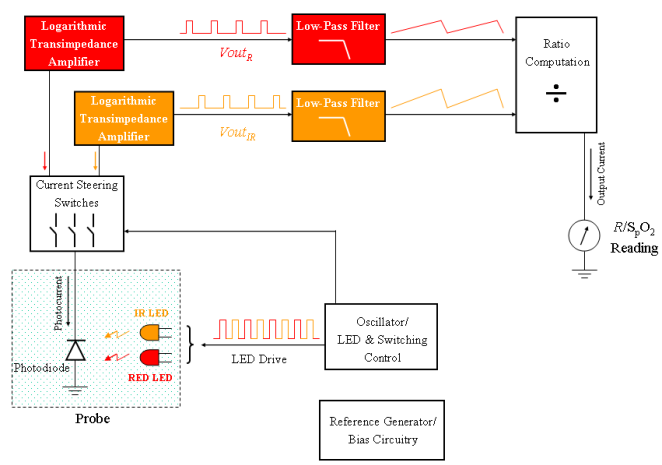


Fig. 4. The architecture of our low-power pulse oximeter

Fig. 5 shows PPG measurements obtained by our pulse oximeter using, as the sensing element, a commercial finger clip transmittance reusable probe manufactured by Nonin Medical, Inc. (model 8000AA), and connected to an healthy subject. We also statistically analyzed the differences between the oxygen saturation readings from our pulse oximeter and a reference oximeter for 11 subjects. Our measured accuracy was –1.2% mean and 1.5% standard deviation, which are

higher than commonly required in medical practice.

Our pulse oximeter was fabricated in an AMI 1.5μm process and has a total power consumption of 4.8mW. State-of-the-art commercial implementations dissipate near 55mW. Our pulse oximeter also performs its entire signal processing in the analog domain, obviating the need for an A-to-D and-DSP and leads to a very area-efficient single-chip system. Simple extensions to our adaptive energy-efficient transimpedance amplifier can lead to sub-milliwatt power consumption without compromising performance [6] and have led to a patent filing that is expected to be published soon.

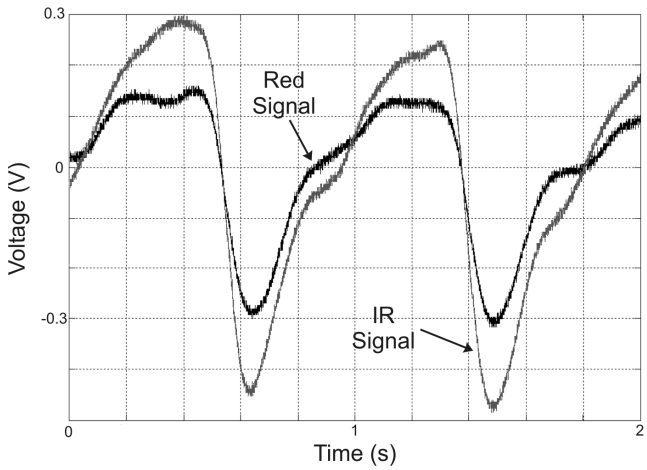


Fig. 5. Pulse-oximeter waveforms captured from a healthy subject.

## IV. An Ultra-Low-Power Phonocardiograph

Phonocardiography (PCG) is the recording of the sounds produced by the heart over time. This method, although diagnostically poor compared with more modern heart analysis techniques, has very important advantages such as being low-cost, low-power, maintenance-free (e.g., no gel is required), robust to 60 Hz pickup, and requiring no electrical contact with the body.

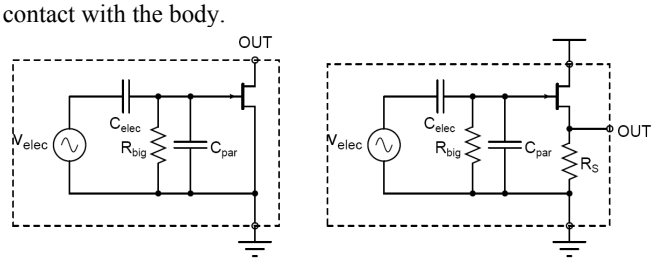


Fig. 6. Circuit diagram of common electret microphones, two-terminal (left) and three-terminal (right).

Microphones can be used to monitor heart sounds. Commercial electret microphones contain built-in low-noise JFETs for buffering. Two configurations, as shown in Fig. 6, are commonly used. In two-terminal microphones, shown on the left, the drain of the n-type JFET, which is normally a depletion-mode device, acts as the output terminal. It is usually connected to an external resistive load, creating a common-source amplifier. The gate voltage is internally tied to ground at DC with the large resistor $R_{big}$, while $C_{par}$ is a small, unwanted parasitic capacitance. The incoming sound pressure wave creates the voltage source $v_{elec}$ in series with the electret capacitance $C_{elec}$. Three-terminal microphones, shown on the right, configure the JFET as a source follower, and are typically more expensive.

Here, we use a two-terminal microphone (Panasonic omnidirectional electret condenser microphone WM-63PR), but replace the resistive load with a programmable current source running off a very low supply voltage to save power. In this regime, the JFET is unsaturated and acts as a voltage-controlled resistor. In this configuration, we can monitor the cardiovascular system with an inexpensive device and at the same time use very little power.

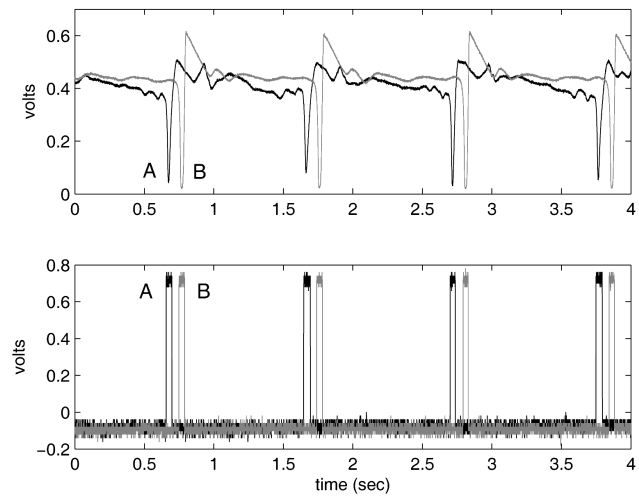


Fig. 7. PCG waveforms measured at neck and wrist.

Measured waveforms are shown in Fig. 7 using a bias current of 30μA and power supply voltage of 0.5V. We have simultaneously measured the sound produced by the blood at the wrist and at the neck of a healthy subject. The bottom part of the picture is the thresholded version of the sound recorded by the microphone. The waveform at the wrist is delayed relative to that at the neck by about 95ms because of the time taken by the systolic pulse to propagate down the length of the arm. This delay can be used to provide information about blood pressure [8]. The continuous monitoring of the blood pressure enabled by this strategy is orders-of-magnitude cheaper in power than a classic method that uses a sphygmomanometer, but calibration techniques are required to get absolute pressure [9].

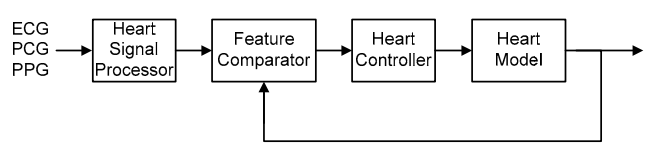


Fig. 8. Concept of the heart locked loop.

## V. An Integrated-Circuit Model of the Heart

As shown in the previous three sections, high power savings can be obtained by carefully designing the analog front-end of medical-monitoring devices. However, this achievement can be lost if a low-power signal-processing strategy is not implemented afterward. In fact, it is a huge waste of power in a wearable system to send the raw signal acquired by the front-end to a base station. The signal needs to be processed as much as possible and only highly significant information should be transmitted. This important goal is extremely difficult to achieve, if only a tiny power budget is available. Here we describe a new approach to this problem that uses an analysis-by-synthesis technique, which potentially requires very little power to operate.

Fig. 8 shows an analysis-by-synthesis block diagram that creates what we term a *"heart locked loop"* (HLL) in analogy with phase locked loops (PLL) used in other communication systems. The heart signal processor transforms ECG, PCG, and PPG information (recorded by the previously explained sensors) to cardiac waveforms that can be compared to those from a heart model via the feature comparator. Errors produced by the comparator are processed by the heart-controller block to update the heart model in a feedback fashion such that it is consistent with the observed data. Eventually, the HLL locks to the input heart signal with optimal cardiovascular parameters output by the controller in a fashion similar to the way a PLL locks to its input. The feature comparator in an HLL is analogous to the phase detector in a PLL, the heart controller in the HLL is analogous to the loop filter in the PLL, and the heart model in the HLL is analogous to the voltage controlled oscillator in the PLL.

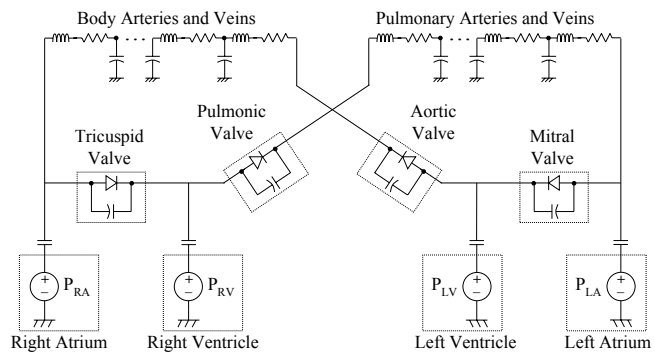


Fig. 9. Electrical model of the human heart.

Combining the HLL with low-power sensors allows the transmission of highly significant cardiovascular parameters, thus saving transmission power. We can even envision the possibility of transmitting information only when some cardiovascular characteristics are not considered normal. To take advantage of such power savings a low-power model of the heart is needed. We have derived an electronic model of the heart using an analogy between mechanical and electronic systems: pressure analogous to voltage, fluid volume velocity analogous to current, and fluid volume analogous to charge [10]. Compliance, inertance, and mechanical damping are then analogous to capacitance, inductance, and electrical resistance. Fig. 9 shows our simplified model of the heart where typical mechanical parameters are converted to electrical parameters. The transmission line comprised of resistors, inductors, and capacitors represents the distributed impedance of the circulatory system. The four valves in the heart are modeled as ideal diodes in parallel with capacitors.

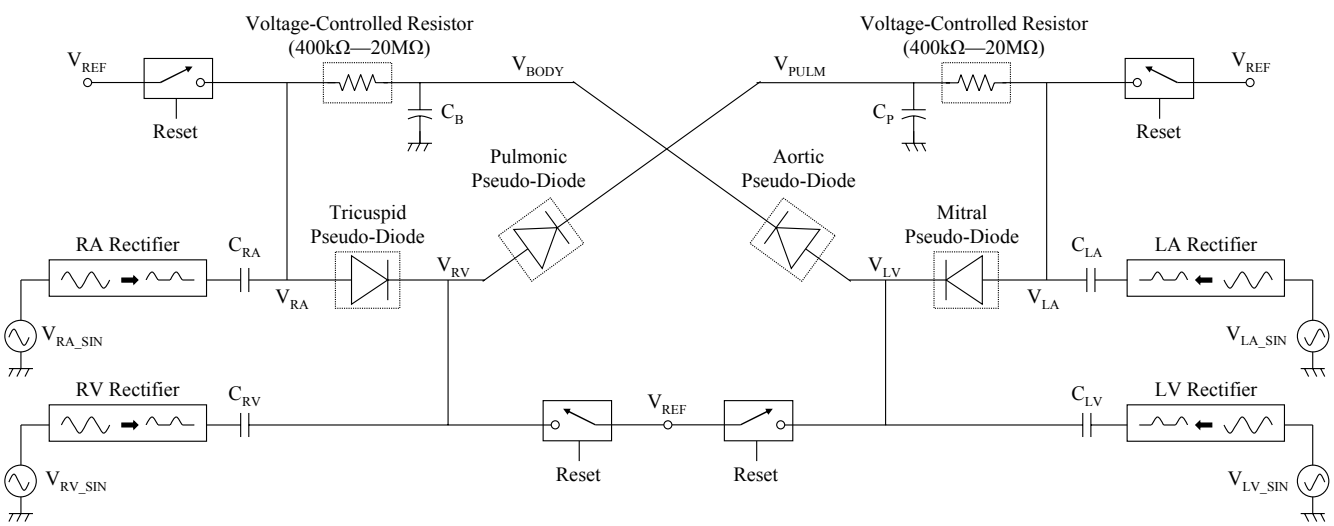


Fig. 10. System schematic for simplified model of the human heart

The model of Fig. 9 was further simplified to the extremely simple one in Fig. 10 [10]. The inductances are not included here, since good accuracy in a heart model is obtained without their use [7]. We have also introduced some reset switches that are not part of the heart model itself, but are used to create an initial condition in the system that allows all of the components to function properly. The value $V_{REF}$ in Fig. 10 corresponds to the average pressure in the cardiovascular system plus an arbitrary offset used so that all components operate within their acceptable common-mode voltage range.

We have developed three ultra-low-power circuits that are equivalent to the basic component types that make up our simplified heart model: pseudo-diodes (zero-threshold diodes), rectifiers, and large voltage-controlled resistors [10]. A chip implementing these circuits was fabricated in an AMI 0.5μm process. Although this chip implements a simplified model of the heart, it reproduces important features of heart function. Fig. 11 shows measured voltage waveforms for the left side of the heart and equivalent pressure values. The most important features present in the real cardiac cycle are simulated by the chip.

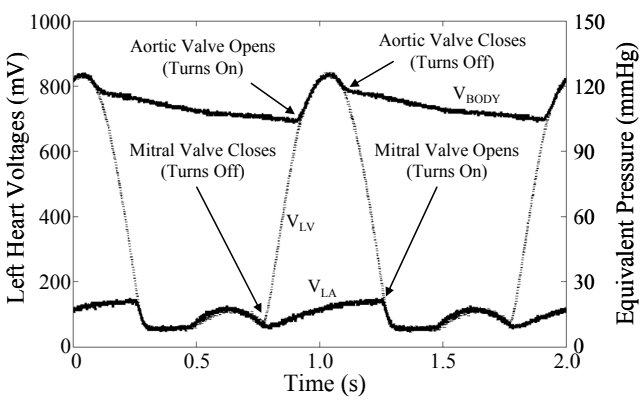


Fig. 11. Measured voltage waveforms for the left half of the heart and equivalent pressure values.

## VI. A Low-Power RF-Energy-Harvesting CMOS Rectifier

A very important component in a medical monitoring device is the power-supply unit. Batteries are the common source of power. However, they are an important bottleneck in the spread of medical-monitoring devices due to their high cost, need of periodic recharges, and limited life span. With the reduction of the overall power needed by our low-power systems, energy-harvesting techniques are a possible solution to battery limitations. Here, we focus on the harvesting of energy with RF-antenna-powered rectifiers since they provide a reliable, low-cost, and low-maintenance method.

Harvesting energy from RF can be efficiently performed using Schottky diodes. Unfortunately, standard CMOS processes generally do not support Schottky diodes. For this reason, we studied all-MOS rectifiers [11]. The most efficient topology found was the self-driven synchronous rectifier shown in Fig. 12. It performs better than diode-based rectifiers when Schottky diodes with low turn-on voltage are not available. In this scheme, $V_P$ and $\overline{V_P}$ are complementary (differential) RF signals from the antenna, and the rectified dc voltage is $V_H - V_L$.

To increase the dc output voltage the rectifier stage can be cascaded in a charge pump-like topology. The RF inputs are fed in parallel into each stage through pump capacitors, and the dc outputs add up in series.

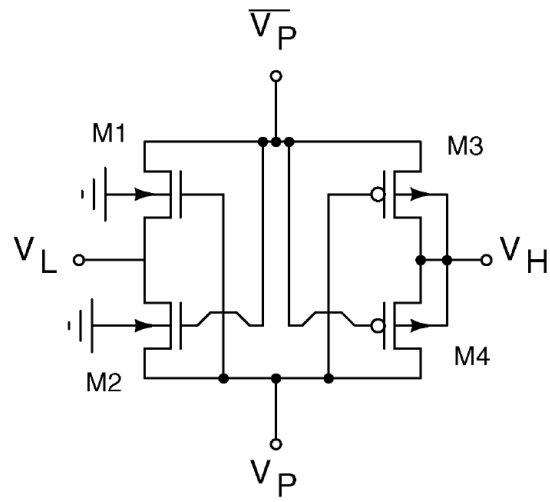


Fig. 12. Four-transistor cell using MOS transistors.

We created an antenna that was impedance matched to the rectifier through two coupled resonators. Two resonators provide about double the matching bandwidth of the commonly-used single resonator. The total size of the antenna is about 2.8''x1.7'', and the simulated gain is 1.5 dBi at 900 MHz. Notice that smaller antenna can be made for 2.4GHz but a lower range will be obtained. Fig. 13 shows the physical structure of the antenna. The antenna is planar and uses a single metal layer on a printed circuit board.

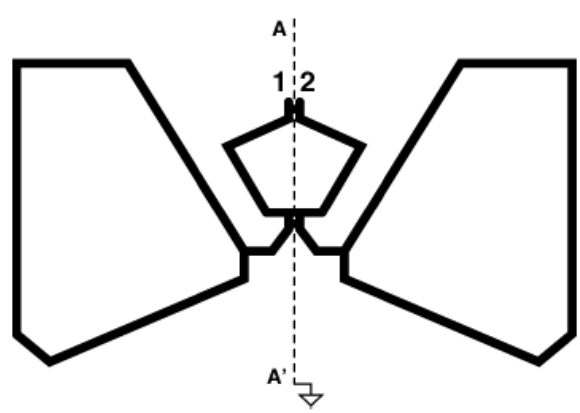


Fig. 13. Physical structure of the final tag antenna. The rectifier chip is fed differentially from ports 1 and 2.

We fabricated a rectifier in standard CMOS processes with 0.18μm minimum feature size with 2 stages. We obtained 23.5% efficiency at 2μW load, which corresponds to an improvement greater than 4x on our own previously published results which, to our best knowledge, are currently the state of the art [11].

## VII. An Ultra-Low-Power Battery-Free Platform for Wireless Medical Monitoring

For building a low-cost, maintenance-free, and lightweight medical monitoring device we need to combine the components illustrated in the previous section. For this purpose, we have developed a wearable battery-free platform for patient-monitoring systems. This platform combines a custom integrated circuit, an antenna for RF energy harvesting, and sensors for monitoring physiological parameters and generating alarms when necessary. The top part of Fig. 14 shows a conceptual view of our platform attached to a flexible, adhesive surface with two microphones and an antenna. At the bottom, the actual experimental 800MHz prototype is visible.

Fig. 15 shows a block diagram of the patient-monitoring chip that we have developed. The chip contains four independently-programmable channels that generate asynchronous event signals when biomedical signals cross a programmable threshold voltage. Event duration and maximum frequency rate are also programmable. Events on different channels can be combined using a programmable logic array (PLA). Each channel can also actuate sensors by supplying DC current. Experimentally, we were able to supply 15μW of power at a distance of 3.1m from an RF source broadcasting 800mW EIRP at 800MHz within a cluttered laboratory environment. Increasing the transmit power to the allowed maximum of 4W should allow a free-space range of 7m (increasable by a factor of 1.4 by using a smaller package for the chip [11]). However, when not powering external sensors, the chip consumes only 1.0μW of power.

Fig. 16 shows an experiment similar to what is described in Section VI. This time, we combined a microphone positioned on the wrist with a pulse oximeter attached to the index finger of a healthy subject. Both outputs were fed into our platform. Fig. 16 shows the measured PCG and PPG waveforms. The peaks in the PPG waveform almost line up with the negative spikes in the PCG because we were recording from adjacent locations, i.e., the pulse propagation delay from the wrist to the finger is small. This small delay is, as explained in Section IV, very useful for measuring the blood pressure of a subject.

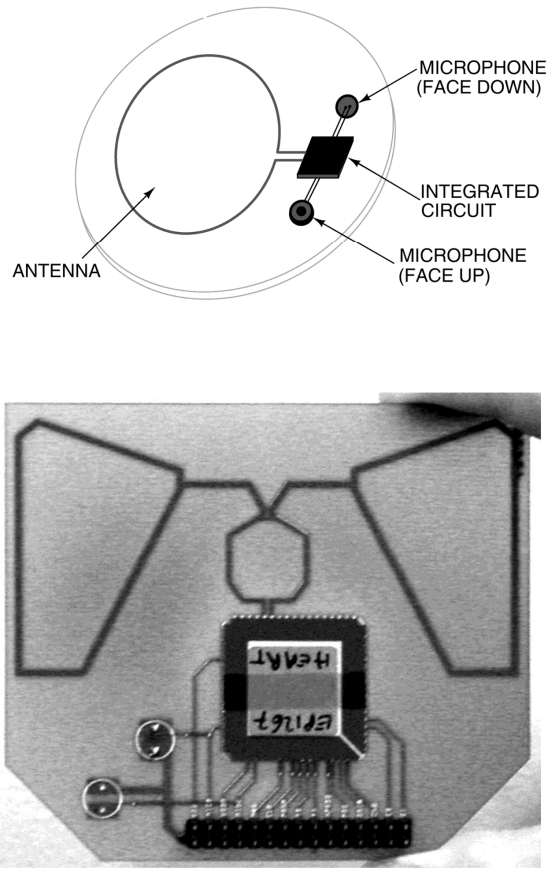


Fig. 14. A battery-free platform.

Medical monitoring sometimes involves the precise localization of patients. This is especially useful in case of emergency where a quick localization of the subject is considered critical or where the robustness of the overall system is achieved using video cameras, which need to be pointed at the subject. For this purpose, we tested our platform using the PCG microphone to receive signals from two small speakers placed at $d$ = 12ft apart using acoustic time-of-flight measurements. The measured microphone positions are shown in Fig. 17 for 9 different positions and 20 trials. We demonstrated that we can localize our platform to within 2 ft (0.6m). Localization is a very important feature that can thus be added to our patient monitor with little power and with low cost.

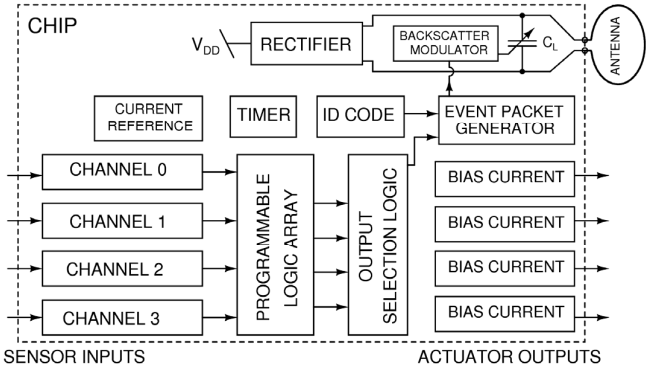


Fig. 15. Block diagram of the low-power patient-monitoring chip.

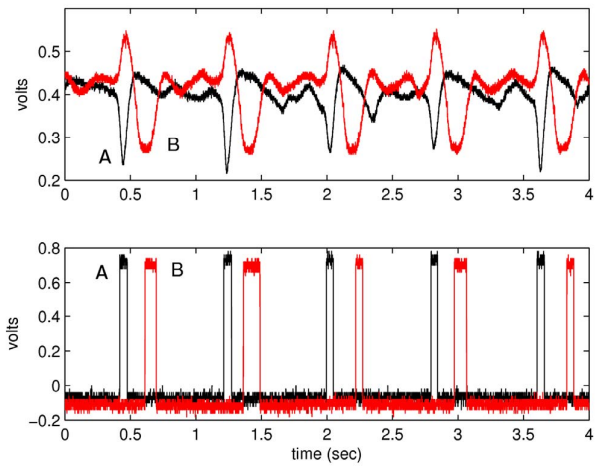


Fig. 16. PCG (A) and PPG (B) waveforms measured at the wrist and fingertip, respectively. Preamplifier (top) and channel (bottom) outputs are shown.

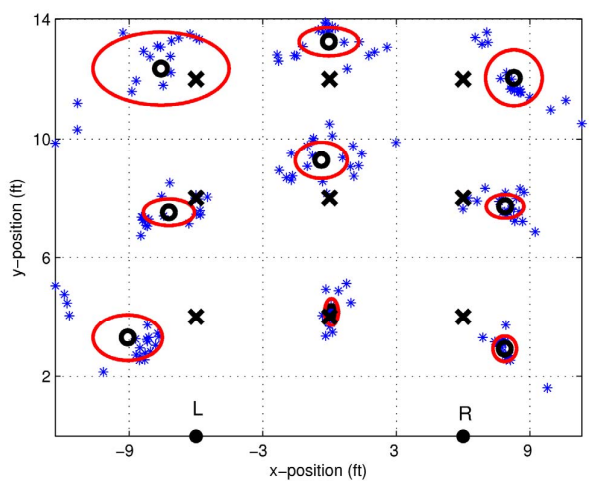


Fig. 17. Localization in two dimensions using acoustic time delays. Measured data points (*), mean positions (○) and standard deviation ellipses are shown for nine cases. Actual positions (×) and the two speakers (●) are also marked.

## VIII. Conclusion

Ultra-low-power non-invasive medical monitoring devices are receiving great attention, not only because they enable medical monitoring in environments where standard equipment is not usable, but also because they are the critical component of home-based telemonitoring services with the potential of great reduction of health care costs.

In this paper, we have presented some innovations toward power reduction for non-invasive medical monitoring devices. In particular, we have described three new ultra-low-power sensor circuits: an electrocardiograph, a pulse oximeter, and a phonocardiograph. In addition, we have introduced an integrated-circuit switched-capacitor model of the heart, a low-power RF-antenna-powered CMOS rectifier, and an ultra-low-power platform for medical monitoring that integrates monitoring circuitry into a wireless battery-free device.

## Acknowledgments

We would also like to thank the MOSIS Educational Program (MEP) for generously providing chip-fabrication resources, the Poitras fellowship program for supporting S. Mandal, and the Office of Naval Research for supporting M. Tavakoli in part.

## References

[1] Y. Ostchega, S.S. Yoon, J. Hughes, T. Louis, "Hypertension awareness, treatment, and control—continued disparities in adults: United States, 2005–2006," *NCHS data brief no Hyattsville, MD: National Center for Health Statistics*, 2008.

[2] "TEN-HMS Study Demonstrates Clinical and Financial Efficacy of Home Telemonitoring," *Philips Medical Systems North America Corporation*, September, 2003.

[3] M. Burke and D. Gleeson, "A micropower dry-electrode ECG preamplifier," *IEEE Transactions on Biomedical Engineering*, Vol. 47, No. 2, pp. 155–162, Feb. 2000.

[4] T. Delbruck and C. Mead, "Adaptive photoreceptor with wide dynamic range," *IEEE International Symposium on Circuits and Systems 1994 (ISCAS '94),* vol. 4, pp. 339–342, Jun 1994.

[5] P. Gray, P. Hurst, S. Lewis, and R. Meyer, "Analysis and Design of Analog Integrated Circuits," Wiley, 2001.

[6] M. Tavakoli, "An Analog VLSI Front End for Pulse Oximetry", Electrical Engineering PhD Thesis supervised by Prof. Sarpeshkar, Massachusetts Institute of Technology, 2005.

[7] T. A. Parlikar, "Modeling and Monitoring of Cardiovascular Dynamics for Patients in Critical Care," PhD Thesis, Electrical Engineering, Massachusetts Institute of Technology, 2007

[8] J. C. Bramwell and A. V. Hill, "The Velocity of the Pulse Wave in Man," *Proc. Royal Society of London - Series B*, vol. 93, no. 652, pp. 298–306, Apr. 1922.

[9] P. Shaltis, A. Reisner, H. Asada, "Calibration of the Photoplethysmogram to Arterial Blood Pressure: Capabilities and Limitations for Continuous Pressure Monitoring," *Proceedings of the 2005 IEEE Engineering in Medicine and Biology 27th Annual Conference (IEEE-EMBS 2005)*, pp. 3970–3973, Shanghai, China, 1-4 September, 2005.

[10] J. Bohorquez, W. Sanchez, L. Turicchia, and R. Sarpeshkar, "An Integrated-Circuit Switched-Capacitor Model and Implementation of the Heart", Invited Paper, *Proceedings of the First International Symposium on Applied Sciences in Biomedical and Communication Technologies (ISABEL)*, pp. 1-5, Aalborg, Denmark, 25-28, October 2008.

[11] S. Mandal, R. Sarpeshkar, "Low-Power CMOS Rectifier Design for RFID Applications" *IEEE Transactions on Circuits and Systems I: Regular Papers*, vol. 54, no. 6, pp.1177–1188, June 2007.

[12] R. Winter and J. Webster, "Reduction of interference due to common mode voltage in biopotential amplifiers," *IEEE Transactions on Biomedical Engineering*, vol. 30, pp. 58–62, 1983.